Critical current improvement and resistance evaluation of superconducting joint between Bi2223 tapes

Y Takeda[1], K Kobayashi[1], A Uchida[1], H Kitaguchi[1], G Nishijima[1], Y Yanagisawa[2], T Nakashima[3], S Yamade[3], S Kobayashi[3], T Kato[3], S Nakamura[4], T Motoki[5] and J Shimoyama[5]

[1] National Institute for Materials Science, 3-13 Sakura, Tsukuba, Ibaraki 305-0003, Japan
[2] RIKEN Center for Biosystems Dynamics Research, 1-7-22, Suehiro-cho, Tsurumi-ku, Yokohama, Kanagawa 230-0045, Japan
[3] Sumitomo Electric Industries, Ltd., 1-1-3 Shimaya, Konohana-ku, Osaka 554-0024, Japan
[4] TEP Co., Ltd., 2-20-4 Kosuge, Katsushika-ku, Tokyo 124-0001, Japan
[5] Department of Physical Sciences, Aoyama Gakuin University, 5-10-1 Fuchinobe, Chuo-ku, Sagamihara, Kanagawa 252-5258, Japan

E-mail: TAKEDA.Yasuaki@nims.go.jp

Received xxxxxx
Accepted for publication xxxxxx
Published xxxxxx

Abstract

We improved the critical current (I_c) of the superconducting joint between the Bi2223 tapes by introducing the two-step sintering process. The in-field transport I_c of ~ 300 A at 4.2 K and 1 T under a 10^{-9} Ω criterion was successfully demonstrated. The I_c improvement can probably be attributed to the enhancement of the intergrain critical current density for a Bi2223 intermediate layer. Ultra-low in-field joint resistance below 10^{-14} Ω at 4.2 K and 1 T was also demonstrated using current decay measurement. To our best knowledge, this study is the first to demonstrate a practical level of in-field transport I_c and ultra-low in-field joint resistance for the superconducting joint between Bi2223 tapes. We believe that this superconducting joint technology will facilitate development of persistent current mode Bi2223 superconducting magnets.

Keywords: HTS, Bi2223, superconducting joint, persistent current mode

1. Introduction

Superconducting joint technology is indispensable for the fabrication of superconducting magnets operated in the persistent current mode, for example, magnets for magnetic resonance imaging (MRI) and nuclear magnetic resonance (NMR) systems. The persistent current mode operation provides magnetic fields with excellent temporal stability. Up to now, conventional metallic low-temperature superconductors (LTSs) have been used for these persistent current mode magnets. The superconducting joint technology for LTS wires with the use of superconducting solders, such as Pb–Bi or Pb–Sn, has already been sufficiently established [1]–[4]. These LTS magnets are usually operated at the liquid He temperature (4.2 K) owing to the low critical

temperature (T_c) of the LTS and superconducting solders at the joints. The magnetic field that LTS magnets can generate at 4.2 K is limited to ~ 23 T because the LTS wire does not have a practical level of critical current density (J_c) above 23 T [5].

To generate high magnetic fields beyond 23 T at 4.2 K, research and development of magnets using cuprate high-temperature superconductors (HTSs) have progressed. The three representative HTSs are $REBa_2Cu_3O_y$ (REBCO, RE = Rare earth) [6], $Bi_2Sr_2CaCu_2O_y$ (Bi2212) [5] and $(Bi,Pb)_2Sr_2Ca_2Cu_3O_y$ (Bi2223) [7]. However, the superconducting joint technology for the HTS conductors had not been established. Joining the HTS conductors was believed to be difficult owing to their short coherence length, large electromagnetic anisotropy, and poor chemical stability [8].

In the last decade, several groups successfully demonstrated superconducting joints between HTS conductors [4],[8]–[16]. Among them, we developed the superconducting joint between Bi2223 tapes [8], which we refer to as the polycrystalline Bi2223 superconducting joint. This is because a polycrystalline Bi2223 intermediate layer is synthesized between two Bi2223 tapes in the joining process.

Ag-sheathed multifilamentary Bi2223 tapes, DI-BSCCO® [7][17], have a high critical current (I_c) above 500 A at 4.2 K under high magnetic fields such as ~ 20 T parallel to the tape surface [18][19]. The tapes have been recently used for magnets that generate high fields beyond 23 T, such as a 1.02 GHz (24.0 T) Bi2223/LTS NMR [20][21] and a 25 T cryogen-free research magnet [22]. The 1.02 GHz NMR magnet was driven with a power supply because the superconducting joint technology for the Bi2223 tapes had not been established.

To form an ideal superconducting joint between Bi2223 tapes, 121 superconducting filaments covered with an Ag matrix must be connected. In our previous study, we successfully exposed almost all of the filaments of the DI-BSCCO® tape in a sufficient connection area [8]. After peeling off the Ag sheath, we carefully polished the tapes with a very small angle (< 1°) against their surface. In the subsequent step used to make a straight lap joint, a polycrystalline Bi2223 thick film [23] was synthesized between the polished surface of two tapes as an intermediate layer. A precursor film was formed on the exposed filaments by dip-coating using the slurry [23]. Uniaxial pressing and sintering were performed under suitable conditions to prepare Bi2223 thick films with a high intergrain J_c. A joint sample fabricated by these processes, where more than 100 filaments were connected, yielded I_c values of 61.4 A and > 400 A at 77 K and 4.2 K, respectively, in self-field [8].

A 1.3 GHz (30.5 T) NMR is being developed [9]. This magnet consists of REBCO, Bi2223, and LTS coils and is designed to be operated in the persistent current mode. The Bi2223 coil comprises more than 40 superconducting joints between the Bi2223 tapes. These joints are placed in a cold space above the coil at low fields below 1 T. For this magnet design, a lap joint with praying hands configuration is planned, where the direction of the current turns over through the joint. An I_c value of the joint (I_{cj}) above 200 A and a joint resistance (R_j) below 10^{-12} Ω per joint at 4.2 K and 1 T are required. However, the superconducting joint between the Bi2223 tapes satisfying these requirements has not been demonstrated so far.

To improve in-field I_{cj}, it is important to enhance the intergrain J_c of the intermediate layer. In our previous study, the J_c of the joint (J_{cj}), which is calculated by dividing I_{cj} by the area of the intermediate layer, was only ~ 400 A cm^{-2} at 4.2 K and self-field [8]. This J_{cj} was approximately one order of magnitude lower than the intergrain J_c of the Bi2223 thick films that we previously developed [23]. This difference is probably attributed to the difference in the fabrication process.

A high-J_c thick film with strong grain coupling is generally fabricated through a conventional two-step sintering process [23]–[25]. This process, which includes intermediate uniaxial pressing and subsequent second sintering, results in both densification and partial *c*-axis grain orientation. Conversely, our previous sample, in which most filaments were connected, was fabricated by the single heat treatment process [8]. This is because the intermediate pressing may have caused mechanical damage of the thin polished tapes without the Ag sheath. To introduce the two-step sintering process including the intermediate pressing, it is necessary to maintain the sufficient mechanical strength of the polished tapes.

In the present study, we fabricated praying-hands-type joint samples. We improved the I_{cj} by introducing the two-step sintering process. We evaluated in-field transport I_{cj} at 4.2 K. We also evaluated in-field R_j at 4.2 K using current decay measurement for a closed loop with the joint.

2. Experimental

Five samples were prepared. The specifications of the samples are listed in Table 1. We used ~ 4.2-mm-wide and ~ 0.22-mm-thick DI-BSCCO® Type H tapes. In practice, the high-strength DI-BSCCO® Type HT-NX tape [18][19][26] with reinforcing Ni-alloy tapes laminated on Type H is used for high field magnets [22]. The reinforcing tapes need to be removed to form the superconducting joint using such high-strength tapes. To avoid additional effects of this process, non-laminated Type H tapes were used in this study.

To maintain sufficient mechanical strength of the polished tapes, we modified the polishing method to expose the filaments. We carefully polished the tapes at an angle of ~ 0.4° against their surface without peeling off the Ag sheath, as shown in Figure 1(a). The Ag sheath was partially

Table 1. Specifications of the tested samples (IP: intermediate pressing at RT and ~ 200 MPa)

Sample	Shape	Heat treatment condition (P_{O2} = 3 kPa, 810°C)	Transport I_{cj} [A] (77 K, self-field)[1)]	Self-inductance, L [μH]
#1	Short praying-hands-type joint (~ 15 cm)	24 h	67	-
#2	Short praying-hands-type joint (~ 15 cm)	24 h	59	-
#3	Short praying-hands-type joint (~ 15 cm)	12 h → IP → 6 h (two-step sintering)	108	-
#4	Short praying-hands-type joint (~ 15 cm)	12 h → IP → 6 h (two-step sintering)	100	-
#5	Closed-loop with praying-hands-type joint (10 cmϕ, five turns)	12 h → IP → 6 h (two-step sintering)	-	5.6

[1)] Transport I_{cj} was determined from a 10^{-9} Ω criterion between the voltage probes in the conventional dc four-probe method.

removed by polishing the tapes. The number of the exposed filaments was ~ 90, as estimated from the geometrical characteristics of the polished tapes and through visual confirmation. This number corresponded to 70–80% of the total number of filaments. The area of the intermediate layer, which covered the exposed filaments as shown in Fig. 1(a), was ~ 70 mm^2.

The joining processes after exposing the filaments were performed in accordance with [8]. The processes include forming a precursor film for an intermediate layer, uniaxial pressing at room temperature (RT) and ~ 200 MPa, and heat treatment under a partial oxygen pressure (P_{O2}) of 3 kPa. P_{O2} was controlled by 3%O_2/Ar gas flow in a tube furnace. Samples were heated to 810°C for 3 h, held for 6–24 h and cooled to RT over ~ 6 h. Each short sample (#1–#4) experienced high temperatures (above 800°C) over the entire section including the tapes. During the heat treatment for the joint of closed-loop sample #5, the folded part (loop part) was held at RT. We confirmed that the I_c degradation of the tape due to heat treatment was sufficiently small, including the temperature transition zone, i.e., the region from high temperature (810°C) to RT. As shown in Table 1, samples #1 and #2 were fabricated via the single heat treatment process. The two-step sintering process, composed of first sintering (12 h), intermediate pressing at RT and ~ 200 MPa, and subsequent second sintering (6 h), was applied to samples #3–#5. Intermediate pressing at ~ 200 MPa is known to be effective to enhance the J_c of a Bi2223 bulk material by densification [25]. To verify reproducibility, we fabricated two short joint samples under each heat treatment condition.

Figure 1(b) shows a schematic of the joint part of praying-hands-type joint samples. To apply uniform pressure to the joint part during uniaxial pressing and fabricate the intermediate layer with a homogeneous thickness, two pieces of polished Bi2223 tape were used as shims. A 30-μm-thick silver foil and a 0.2-mm-thick metal cap were set for the protection and reinforcement of the joint part, respectively.

The microstructure of the joint part was observed via field emission scanning electron microscopy (FE-SEM, Carl Zeiss AG-ULTRA55). The observed positions are shown in Fig. 1(b).

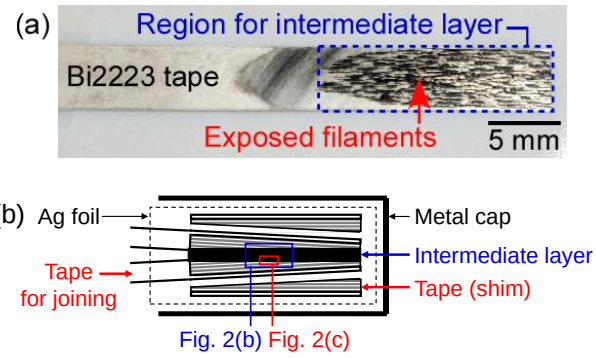

Figure 1. (a) Photograph of a tape polished at a small angle (~ 0.4°) without peeling off the Ag sheath. The region forming the intermediate layer in the joining process is also shown. (b) Schematic of the joint part of the praying-hands-type joint. The positions for microstructural observation are also shown.

Transport measurements for samples #1–#4 were performed in a liquid N_2 bath (77 K) and liquid He bath (4.2 K) using the conventional dc four-probe method. I_{cj} was determined from a resistance criterion of 10^{-9} Ω between the voltage probes. In the measurements at 4.2 K, a magnetic field was applied parallel to the tape surface.

R_j at 4.2 K was evaluated with the use of a recently developed superconducting joint resistance evaluation system [27]. We carefully performed current decay measurement for a closed-loop sample #5. The current in the loop (I_{loop}) was estimated using a Hall sensor. The Hall sensor was installed close to the tapes of sample #5 rather than at the coil center to increase the measurement sensitivity [27]. We calibrated the Hall sensor using the current before measurement and confirmed linearity between Hall sensor output voltage and I_{loop}. The coefficient was used to estimate I_{loop}. An external magnetic field of 1 T parallel to the tape surface was applied only at the joint.

3. Results and discussion

Figure 2(a) shows a photograph of praying-hands-type joint sample #1. Figs. 2(b) and 2(c) show backscattered electron images of the longitudinal cross-section of the joint

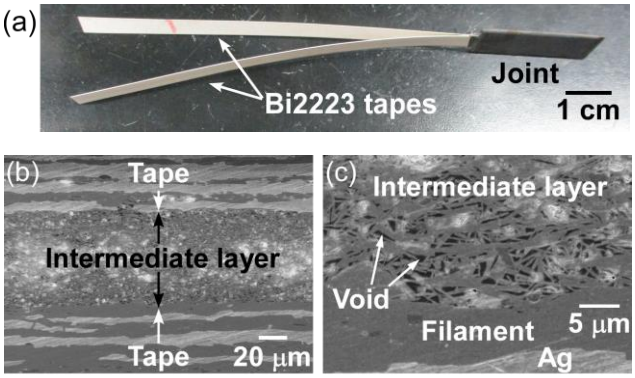

Figure 2. (a) Photograph of praying-hands-type joint sample #1. (b, c) Backscattered electron images for the longitudinal cross-section of the joint part of sample #1. The observed positions are shown in Figure 1(b).

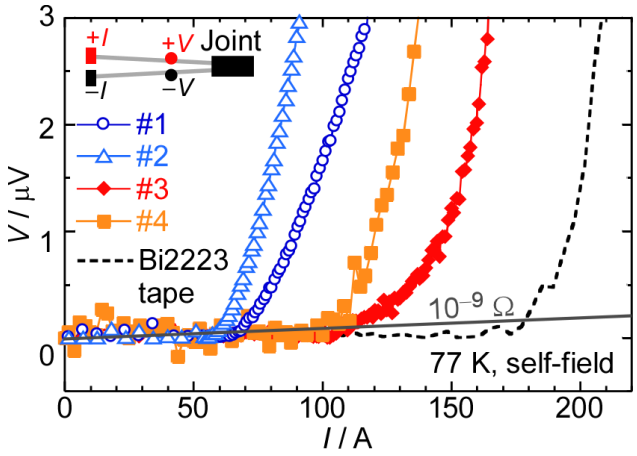

Figure 3. *V–I* curves measured at 77 K in self-field for samples #1–#4 and Bi2223 tape (DI-BSCCO®, without joint). The line at 10^{-9} Ω for determining I_{cj} is also shown.

part of sample #1. From Fig. 2(b), it is observed that the intermediate layer with a homogenous thickness of ~ 100 μm was formed. A large number of voids were observed in the intermediate layer, as shown in Fig. 2(c). Conversely, at the interface between the intermediate layer and one of the filaments the crystals were in good contact.

Figure 3 shows the *V–I* curves for samples #1–#4 at 77 K in self-field. A *V–I* curve of a Bi2223 tape (DI-BSCCO®, without joint) for comparison and the line at 10^{-9} Ω for determining I_{cj} are also shown. The voltage of each joint sample as well as that of the tape were below the measurement limit up to a certain current. Nonlinear voltage rise, i.e., the general superconducting-to-normal transition was observed in each sample and the tape. These results imply that the superconducting joint was formed in each sample. The I_{cj} values for samples #1 #2, #3, and #4 were 67, 59, 108, and 100 A, respectively, as summarized in Table I. The I_{cj} values for samples fabricated under the same condition were comparable with a variance of ~ 10%. This implies that the I_{cj} reproducibility of this superconducting joint technology is sufficiently high.

The I_{cj} values for praying-hands-type joint samples #1 and #2 were comparable to that of the straight lap joint in our previous study (61 A) [8]. This is because samples #1 and #2 were fabricated by the same single heat treatment condition as the straight lap joint. Conversely, the values of I_{cj} for samples #3 and #4 were remarkably higher (> 1.5 times) than those for samples #1 and #2. This I_{cj} improvement is probably attributed to the enhancement of the intergrain J_c for the intermediate layer by densification, which was achieved by introducing the two-step sintering process [25].

Notably, even the highest I_{cj} value (sample #3) is only 60% of the I_c value for the tape of 180 A. The I_{cj} value was probably suppressed by the small number of the connected filaments and insufficient intergrain J_c at the joint interface. In addition, we cannot deny the possibility that the I_c value of the tapes in each sample was degraded through the joining process. We confirmed that the I_c of the tape was degraded by mechanical damage to the filaments through uniaxial pressing. The filament damage can be healed during the heat treatment for joining [28]. This probably led to recovering the degraded I_c, although we have not evaluated the degree of recovery quantitatively. To achieve an I_{cj} comparable to the I_c of the tape, optimization of the fabrication conditions considering the above may be necessary.

The magnetic field dependences of the transport I_{cj} value for samples #1 and #3 at 4.2 K are shown in Figure 4. The magnetic field was increased in intervals up to 2 T. The inset in Fig. 4 shows the *V–I* curves for #3 at 4.2 K and 1 T with the line at 10^{-9} Ω. The measurements for sample #3 were performed twice to verify the reproducibility, as denoted by the arrows in Fig. 4. The two I_{cj}–*H* curves for #3 were in good agreement. As shown in the inset, the reproducible *V–I* curves for sample #3 were observed. This indicates the mechanical robustness of the joint against the electromagnetic force through the in-field transport measurements. We confirmed the *n*-value in the power-*n* model [4] to be ~ 20 at 4.2 K and 1 T in the voltage region below 0.2 μV.

I_{cj} for #1 and #3 were 259 and 708 A at 0.2 T, 103 and 290–306 A at 1 T, respectively. A higher in-field I_{cj} value at 4.2 K for sample #3 than for sample #1 was observed, as well as a higher self-field I_{cj} value at 77 K for sample #3. This is probably because of the enhancement of the intergrain J_c of the intermediate layer. The value of I_{cj} of 290–306 A at 4.2 K and 1 T sufficiently satisfies the design requirement of the 1.3 GHz NMR magnet [9]. However, the J_{cj} value of sample #3 is only ~ 1 kA cm^{-2} at 0.2 T. This suggests that even the intermediate layer of sample #3 had a lower intergrain J_c than that of the thick film previously

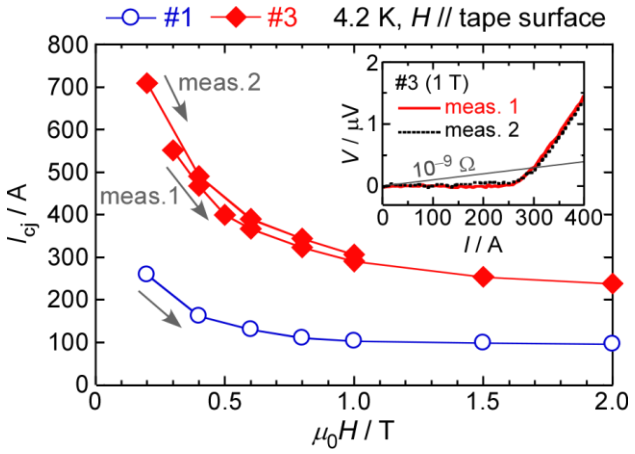

Figure 4. Magnetic field dependence of transport I_{cj} for samples #1 and #3 at 4.2 K. The magnetic field was applied parallel to the tape surface and increased in steps. Measurement for #3 was performed twice, as denoted by the arrows. An inset shows *V*–*I* curves for sample #3 at 4.2 K and 1 T. I_{cj} was determined by the 10^{-9} Ω criterion shown in the inset.

reported (~ 50 kA cm^{-2} at 4.2 K in self-field) [23]. Clarification of the quantitative relationship between the intergrain J_c of the intermediate layer and I_{cj} is in progress and will be reported elsewhere. We believe that there is considerable room for improving I_{cj} by strengthening grain coupling. Grain alignment and control of the chemical compositions is probably effective to enhance J_{cj}, as revealed in our studies for the Bi2223 polycrystalline bulks or thick films with high intergrain J_c [23][29][30].

Current decay measurement for a five-turn closed-loop sample #5 with the praying-hands-type joint shown in Figure 5(a) was performed. Given that sample #5 was closed-loop using a brittle DI-BSSCO® Type H tape and that transport measurements might have damaged the sample by overcurrent or attaching the current leads and voltage probes, we did not measure I_{cj}. Fig. 5(b) shows the result of the measurement at 4.2 K and 1 T. I_{loop} (normalized) was calculated by dividing I_{loop} by I_{loop} (t = 0), which is the maximum value of I_{loop}. The I_{loop} injected at t = 0 was ~ 140 A, and a remarkably slow decay of I_{loop} was observed. We estimated the resistance of the closed-loop circuit (R) by fitting the decay curve using a self-inductance (L) of 5.6 μH and a decay function of $I_{loop} = A \exp((-R / L)\, t)$, where A is an arbitrary constant. From the fitting of experimental data points between 4×10^4 and 7×10^4 s, R was deduced to be 3.8×10^{-15} Ω. Although R is determined by several factors other than R_j such as the flux creep and effect of the screening current, we can conclude that R_j is below 10^{-14} Ω. Thus, the polycrystalline Bi2223 superconducting joint that we developed fully satisfied the design requirements of the 1.3 GHz NMR magnet [9].

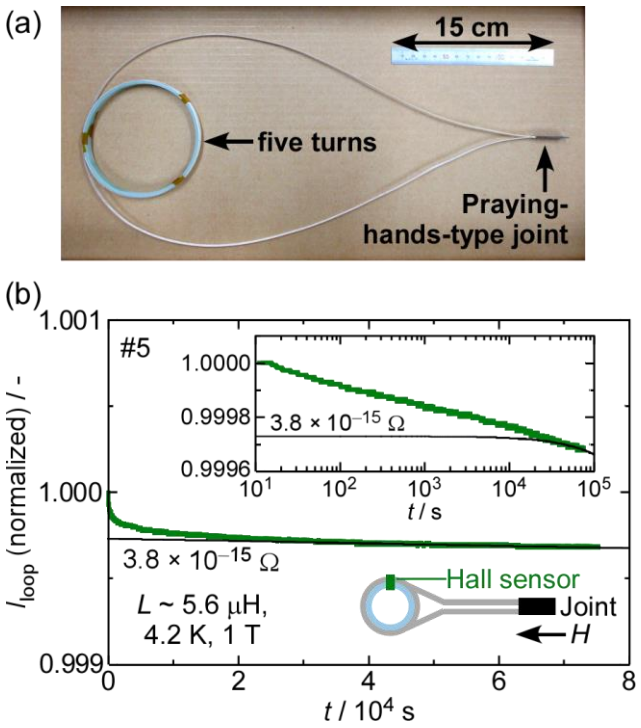

Figure 5. (a) Photograph of closed-loop sample #5. (b) Result of current decay measurement for sample #5 at 4.2 K with an exponential decay curve corresponding to 3.8×10^{-15} Ω, which was deduced from the fitting of experimental data points between 4×10^4 and 7×10^4 s. An inset shows a magnified view of the fitting on a log scale. An external magnetic field of 1 T parallel to the tape surface was applied only at the joint. I_{loop} was injected at t = 0 and estimated to be ~ 140 A with the use of a Hall sensor installed close to the tapes of sample #5.

Thus, we demonstrated transport I_{cj} improvement and R_j evaluation for the polycrystalline Bi2223 superconducting joint. To our best knowledge, this study is the first to demonstrate a practical level of in-field transport I_{cj} and ultra-low in-field R_j below 10^{-14} Ω for the superconducting joint between Bi2223 tapes. We believe that this superconducting joint technology enables persistent current mode Bi2223 superconducting magnets.

4. Summary

We improved I_{cj} of the polycrystalline Bi2223 superconducting joint by introducing a two-step sintering process. This I_{cj} improvement can probably be attributed to the enhancement of the intergrain J_c of the intermediate layer. The transport I_{cj} of ~ 300 A and ultra-low R_j below 10^{-14} Ω at 4.2 K and 1 T were successfully demonstrated. We believe that this superconducting joint technology will facilitate the development of persistent current mode Bi2223 superconducting magnets.

Acknowledgements

This work was supported by JST Mirai-Program Grant Number JPMJMI17A2 and Special Postdoctoral Researcher Program at RIKEN, Japan. The microstructural observation in this work was supported by Center for Instrumental Analysis, College of Science and Engineering, Aoyama Gakuin University.

References

[1] Thornton R F 1986 Superconducting joint for superconducting wires and coils and method of forming *US Patent* 4744506

[2] Swenson C A and Markiewicz W D 1999 Persistent Joint Development for High Field NMR *IEEE Trans. Appl. Supercond.* **9** 185–188

[3] Kodama M, Okamoto K, Koga Y, Yamamoto T and Watanabe H 2015 Analysis for formation of current path in the superconducting joint between Nb-Ti wires with the solder matrix replacement method *Supercond. Sci. Technol.* **28** 045019

[4] Brittles G D, Mousavi T, Grovenor C R M, Aksoy C and Speller S C 2015 Persistent current joints between technological superconductors *Supercond. Sci. Technol.* **28** 093001

[5] Larbalestier D C, Jiang J, Trociewitz U P, Kametani F, Scheuerlein C, Dalban-Canassy M, Matras M, Chen P, Craig N C, Lee P J and Hellstrom E E 2014 Isotropic round-wire multifilament cuprate superconductor for generation of magnetic fields above 30 T *Nat. Mater.* **13** 375–381

[6] Senatore C, Barth C, Bonura M, Kulich M and Mondonico G 2016 Field and temperature scaling of the critical current density in commercial REBCO coated conductors *Supercond. Sci. Technol.* **29** 014002

[7] Sato K, Kobayashi S and Nakashima T 2012 Present Status and Future Perspective of Bismuth-Based High-Temperature Superconducting Wires Realizing Application Systems *Jpn. J. Appl. Phys.* **51** 010006

[8] Takeda Y, Motoki T, Kitaguchi H, Nakashima T, Kobayashi S, Kato T and Shimoyama J 2019 High I_c superconducting joint between Bi2223 tapes *Appl. Phys. Express* **12** 023003

[9] Maeda H, Shimoyama J, Yanagisawa Y, Ishii Y and Tomita M 2019 The MIRAI Program and the New Super-High Field NMR Initiative and Its Relevance to the Development of Superconducting joints in Japan *IEEE Trans. Appl. Supercond.* **29** 4602409

[10] Park Y, Lee M, Ann H, Choi Y H and Lee H 2014 A superconducting joint for $GdBa_2Cu_3O_{7-\delta}$-coated conductors, *NPG Asia Mater.* **6** e98

[11] Jin X, Yanagisawa Y, Maeda H and Takano Y 2015 Development of a superconducting joint between a $GdBa_2Cu_3O_{7-\delta}$-coated conductor and $YBa_2Cu_3O_{7-\delta}$ bulk: towards a superconducting joint between RE (Rare Earth) $Ba_2Cu_3O_{7-\delta}$-coated conductors *Supercond. Sci. Technol.* **28** 075010

[12] Ohki K, Nagaishi T, Kato T, Yokoe D, Hirayama T, Ikuhara Y, Ueno T, Yamagishi K, Takao T, Piao R, Maeda H and Yanagisawa Y 2017 Fabrication, microstructure and persistent current measurement of an intermediate grown superconducting (iGS) joint between REBCO-coated conductors *Supercond. Sci. Technol.* **30** 115017

[13] Chen P, Trociewitz U P, Davis D S, Bosque E S, Hilton D K, Kim Y, Abraimov D V, Starch W L, Jiang J, Hellstrom E E and Larbalestier D C 2017 Development of a persistent superconducting joint between Bi-2212/Ag-alloy multifilamentary round wires *Supercond. Sci. Technol.* **30** 025020

[14] Mukoyama S, Nakai A, Sakamoto H, Matsumoto S, Nishijima G, Hamada M, Saito K and Miyoshi Y 2018 Superconducting joint of REBCO wires for MRI magnet *J. Phys.: Conf. Ser.* **1054** 012038

[15] Jin X, Suetomi Y, Piao R, Matsutake Y, Yagai T, Mochida H, Yanagisawa Y and Maeda H 2019 Superconducting joint between multi-filamentary $Bi_2Sr_2Ca_2Cu_3O_{10+\delta}$ tapes based on incongruent melting for NMR and MRI applications *Supercond. Sci. Technol.* **32** 035011

[16] Mousavi T, Santra S, Melhem Z, Speller S and Grovenor C 2021 Superconducting Joint Structures For Bi-2212 Wires Using a Powder-in-Tube Technique *IEEE Trans. Appl. Supercond.* **31** 6400504

[17] Ayai N, Kato T, Fujikami J, Kobayashi S, Kikuchi M, Yamazaki K, Yamade S, Ishida T, Tatamidani K, Hayashi K, Sato K, Hata R, Kitaguchi H, Kumakura H, Osamura K and Shimoyama J 2008 DI-BSCCO wire with I_c over 200 A at 77 K *J. Phys.: Conf. Ser.* **97** 012112

[18] Miyoshi Y, Nishijima G, Kitaguchi H and Chaud X 2015 High field I_c characterizations of commercial HTS conductors *Physica C* **516** 31–35

[19] Bonura M, Barth C and Senatore C 2019 Electrical and Thermo-Physical Properties of Ni-Alloy Reinforced Bi-2223 Conductors *IEEE Trans. Appl. Supercond.* **29** 6400205

[20] Hashi K, Ohki S, Matsumoto S, Nishijima G, Goto A, Deguchi K, Yamada K, Noguchi T, Sakai S, Takahashi M, Yanagisawa Y, Iguchi S, Yamazaki T, Maeda H, Tanaka R, Nemoto T, Suematsu H, Miki T, Saito K and Shimizu T 2015 Achievement of 1020 MHz NMR *J. Magn. Reson.* **256** 30–33

[21] Nishijima G, Matsumoto S, Hashi K, Ohki S, Goto A, Noguchi T, Iguchi S, Yanagisawa Y, Takahashi M, Maeda H, Miki T, Saito K, Tanaka R and Shimizu T 2016 Successful Upgrading of 920-MHz NMR Superconducting Magnet to 1020 MHz Using Bi-2223 Innermost Coil *IEEE Trans. Appl. Supercond.* **26** 4303007

[22] Awaji S, Watanabe K, Oguro H, Miyazaki H, Hanai S, Tosaka T and Ioka S 2017 First performance test of a 25 T cryogen-free superconducting magnet *Supercond. Sci. Technol.* **30** 065001

[23] Takeda Y, Shimoyama J, Motoki T, Nakamura S, Nakashima T, Kobayashi S and Kato T 2018 Development of high J_c Bi2223/Ag thick film materials prepared by heat treatment under low P_{O2} *Supercond. Sci. Technol.* **31** 074002

[24] Asano T, Tanaka Y, Fukutomi M, Jikihara K, Machida J and Maeda H 1988 Preparation of Highly Oriented Microstructure in the (Bi, Pb)-Sr-Ca-Cu-O Sintered Oxide Superconductor *Jpn. J. Appl. Phys.* **27** L1652–L1654

[25] Ito A, Matsuda M, Iwai Y, Ishii M, Takata M, Yamashita T and Koinuma H 1989 Influence of Intermediate Pressing on Superconducting Characteristics in Bi-Pb-Sr-Ca-Cu-O System *Jpn. J. Appl. Phys.* **28** L380–L381

[26] Nakashima T, Yamazaki K, Kobayashi S, Kagiyama T, Kikuchi M, Takeda S, Osabe G, Fujikami J and Osamura K

2015 Drastic Improvement in Mechanical Properties of DI-BSCCO Wire With Novel Lamination Material *IEEE Trans. Appl. Supercond.* **25** 6400705

[27] Kobayashi K, Nishijima G, Uchida A, Amaya M, Banno N and Kitaguchi H 2020 Development of a Superconducting Joint Resistance Evaluation System *IEEE Trans. Appl. Supercond.* **30** 9000204

[28] Parrell J A, Polyanskii A A, Pashitski A E and Larbalestier D C 1996 Direct evidence for residual, preferentially-oriented cracks in rolled and pressed Ag-clad BSCCO tapes and their effect on the critical current density *Supercond. Sci. Technol.* **9** 393–398

[29] Takeda Y, Shimoyama J, Motoki T, Kishio K, Nakashima T, Kagiyama T, Kobayashi S and Hayashi K 2017 Fabrication of Bi2223 bulks with high critical current properties sintered in Ag tubes *Physica C: Supercond.* **534** 9–12

[30] Takeda Y, Iwami T, Saito Y, Motoki T and Shimoyama J 2021 Fabrication of high J_c Bi2223 thick films through grain alignment technique using a permanent magnet *Physica C: Supercond.* **584** 1353873

